International Journal of Power Electronics and Drive System (IJPEDS)
Vol. 11, No. 1, March 2020, pp. 10~23
ISSN: 2088-8694, DOI: 10.11591/ijpeds.v11.i1.pp10-23

Performance enhancements of DFIG wind turbine using fuzzy-feedback linearization controller augmented by high-gain observer

Kada Boureguig[1], Abdellah Mansouri[2], Ahmed Chouya[3]
[1] Oran University of Science and Technology - Mohamed Boudiaf USTO-MB, Algeria
[2] National Polytechnic University Oran, Algeria
[3] Department of Electrical Engineering, Djillali Bounaama University, Algeria

Article Info

Article history:

Received Apr 17, 2019
Revised Jul 22, 2019
Accepted Aug 12, 2019

Keywords:

DFIG
Feedback linearization control
Fuzzy logic
High gain observer
Lyapunov stability

ABSTRACT

This paper proposes a feedback linearization control of doubly fed induction generator based wind energy systems for improving decoupled control of the active and reactive powers stator. In order to enhance dynamic performance of the controller studied, the adopted control is reinforced by a fuzzy logic controller. This approach is designed without any model of rotor flux estimation. The difficulty of measuring of rotor flux is overcome by using high gain observer. The stability of the nonlinear observer is proved by the Lyapunov theory. Numerical simulations using MATLAB-SIMULINK shown clearly the robustness of the proposed control, particularly to the disturbance rejection and parametric variations compared with the conventional method.

Corresponding Author:

Kada Boureguig,
Oran University of Science and Technology - Mohamed Boudiaf,
USTO-MB, BP 1505 El M'Naouer, 31000 Oran, Algeria.
Email: kada.boureguig@univ-usto.dz

1. INTRODUCTION

The wind energy is a pollution-free and effective source. Therefore, a wind power generation system becomes one of the potential sources of alternative energy for the future [1]. Energy consumption over the last century has increased significantly due to the great industrialization. Recently, particular interest has been given to generating electricity from renewable energy sources. Of all renewable sources, wind energy holds the largest market share and is expected to maintain rapid growth in the coming years [2]. Wind energy systems have received considerable attention over the past decade as one of the most promising renewable energy sources due to negative environmental influences and the high cost of conventional energy sources. In this context, several countries have turned to explore the wind energy sector, leading researchers to conduct research to improve the efficiency and power of electromechanical conversion and quality of providing energy [3].To meet energy needs, it is imperative to find adjusted and flexible solutions by reducing energy consumption or increasing energy production by adding power plants or improving the efficiency of existing installations. In addition, the dynamic improvement of the performance of renewable energy systems, whose non-linear characteristics are particularly important, especially with the rapid growth of their use. Therefore, the control of the Wind Power Conversion System (WECS) based on doubly feed induction generator (DFIG) with intermittent input wind speed is particular interest in the energy and control communities. DFIGs are potential candidates for high power wind systems because they can generate reactive current and

produce constant frequency power for variable speed operation. However, the main disadvantage of the DFIG is its brushes and slip rings structure, which involves permanent maintenance and reduces the life time of the machine [4]. This type of generators has been widely used for wind systems [5]. The control and operation of these systems has been the subject of many research projects in recent years [6]. In this perspective, various studies have been proposed in [7-9] to control wind turbine systems based DFIG from the classical configurations by application of Field oriented control (FOC) strategy. However, the WT-DFIG is highly nonlinear system, with strong couplings between the different variables of the systems.

In this context, many nonlinear control methods have been developed. Penghan Li et al [10] proposes a non linear controller based on state feedback linearization strategy to reduce sub-synchronous control interaction inseries-compensated doubly fed induction generator (DFIG)-based wind power plants.

In [11] the authors have used a robust nonlinear feedback linearization controller based sliding mode control to relieve sub-synchronous control interaction in doubly-fed induction generator based wind farms connected to series-compensated transmission lines. The two aforementioned works show good performances. However, the authors did not use a nonlinear model and DFIG Wind Turbine control scheme is based on vector control. In addition, the states of the DFIG are supposed to be measured.

Djillali et al [12] have used Neural Input-Output Feedback Linearization Control. The neural controller is based on a Recurrent High Order Neural Network, trained with an Extended Kalman Filter. This last method uses a simple PI controller to define the control law defined by a relationship linking the new internal inputs to the physical inputs. The same strategy control has been applied in [13] based on the linear quadratic regulator (LQR). Due to the limitations presented by the two linear controllers the PI and the LQR which have a low robustness to parameter variations as well as to unbalanced grid voltage which have direct effects on the dynamic performance of the system, and poses serious problems, such as oscillations of the stator power and the generator torque, which are detrimental to the mechanical system and the electrical network [14].

In this paper the Feedback linearization technique is combined with Fuzzy logic to form Fuzzy-Feedback Linearization Controller applied to a non-linear model of DFIG to improve the performance of the system such as the response time , robustness against parameter variations and the sensitivity to perturbations (unbalanced grid voltage) .This new method is augmented by High Gain Observer (HGO) mainly used to estimate generator rotor flux, based on the measurement of rotor currents ,stator voltages and the mechanical speed. The effectiveness of the proposed controller is compared to the conventional Feedback linearization control by simulation results in Matlab Simulink.

2. MODELING OF STUDIED SYSTEM

As shown in Figure 1 the system is composed of two parts; the first is the conversion of the kinetic energy of the wind into mechanical energy via a turbine and the second is the conversion of the mechanical energy at the level of the turbine shaft into electrical energy via a double-feed generator. The stator is connected directly to the grid and its rotor also via a static converter which allows delivering the necessary control voltages of the stator powers.

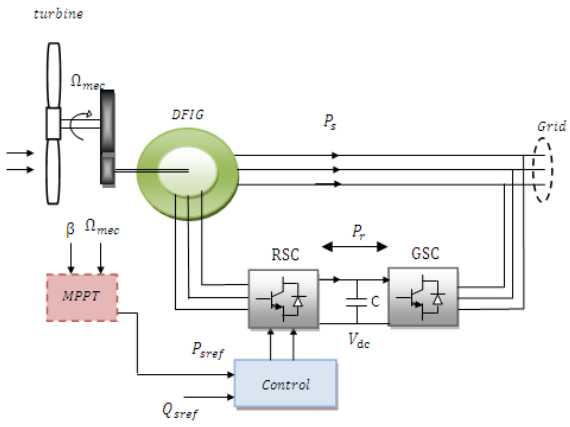

Figure1. System under study

2.1. Turbine model

The aerodynamic power appearing at the rotor of the turbine is then written [15].

$$P_t = \frac{1}{2}\rho C_P(\lambda,\beta)SV^3 \quad (1)$$

Where: ρ is the air density and S the swept surface area of the turbine (πR^2)

V is the wind speed (m/s), $C_P(\lambda,\beta)$ is the power coefficient of the turbine, λ is the tip speed ratio and β is the pitch angle. The tip speed ratio is:

$$\lambda = \frac{R\omega_t}{V} \quad (2)$$

where: R is the radius of the turbine (m) and ω_t is the speed turbine (rad/s).Figure 2 shows the curve of the power coefficient versus λ for a constant value of the pitch angle β.

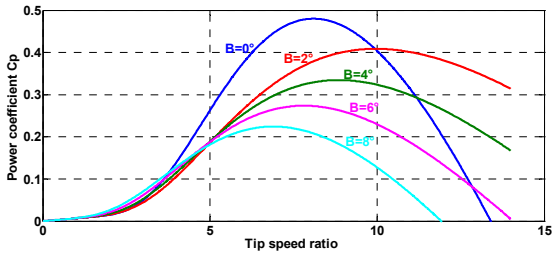

Figure 2.Typical curve of power coefficient.

2.2. Dynamique model of DFIG

The mathematical models of three DFIG phases in the Park frame are written as follows [16]:

$$\begin{cases} v_{ds} = R_s i_{ds} + \frac{d\varphi_{ds}}{dt} - \omega_s \varphi_{qs} \\ v_{qs} = R_s i_{qs} + \frac{d\varphi_{qs}}{dt} + \omega_s \varphi_{ds} \\ v_{dr} = R_r i_{dr} + \frac{d\varphi_{dr}}{dt} - (\omega_s - \omega)\varphi_{qr} \\ v_{qr} = R_r i_{qr} + \frac{d\varphi_{qr}}{dt} + (\omega_s - \omega)\varphi_{dr} \end{cases} \quad (3)$$

$$\begin{cases} \varphi_{ds} = L_s i_{ds} + M i_{dr} \\ \varphi_{qs} = L_s i_{qs} + M i_{qr} \\ \varphi_{dr} = L_r i_{dr} + M i_{ds} \\ \varphi_{qr} = L_r i_{qr} + M i_{qs} \end{cases} \quad (4)$$

Where R_r, $R_s$are the rotor and stator resistances, respectively; L_s, L_r, M are the rotor, stator and mutual inductances, respectively; i_{ds-r} , $i_{qs-r}$are the stator–rotor current components; v_{ds-r} , $v_{qs-r}$are the components of the stator–rotor voltage; φ_{ds-r} , $\varphi_{qs-r}$are the stator–rotor flux components; ω , ω_s are the rotating and stator pulsations, respectively.

The model of DFIG according to the rotor components is represented by the following equations [15].

$$\begin{cases} \frac{di_{dr}}{dt} = -a_1 i_{dr} + \omega_s i_{qr} + a_2 \varphi_{dr} - a_3 \omega \varphi_{qr} - a_4 v_{ds} + a_3 v_{dr} \\ \frac{di_{qr}}{dt} = -\omega_s i_{dr} - a_1 i_{qr} + a_2 \varphi_{qr} + a_3 \omega \varphi_{dr} - a_4 v_{qs} + a_3 v_{qr} \\ \frac{d\varphi_{dr}}{dt} = -R_r i_{dr} + \omega_s \varphi_{qr} - \omega \varphi_{qr} + v_{dr} \\ \frac{d\varphi_{qr}}{dt} = -R_r i_{qr} - \omega_s \varphi_{dr} + \omega \varphi_{dr} + v_{qr} \end{cases} \quad (5)$$

where

$a_1 = (\frac{1}{\sigma T_r} + \frac{1}{\sigma T_s})$, $a_2 = \frac{1}{\sigma L_r T_s}$, $a_3 = \frac{1}{\sigma L_r}$,$a_4 = \frac{1-\sigma}{\sigma M}$,$\sigma = 1 - \frac{1-M^2}{L_s L_r}$, $b = R_r$,
$C_1 = \frac{p^2}{j}$, $C_2 = \frac{P}{j}$, $T_s = \frac{L_s}{R_s}$, $T_r = \frac{L_r}{R_r}$
σ is the dispersion coefficient
The electromechanical dynamic equation is then given by

$$\frac{d\omega}{dt} = \frac{P^2}{J}\left(\varphi_{qr} i_{dr} - \varphi_{dr} i_{qr}\right) + \frac{P}{j}(C_{vis} + C_G) \quad (6)$$

where P is the number of pole pairs; J is the inertia of the shaft , C_G is the torque on the generator .All frictions on this shaft are included in C_{vis}.

We put

$\left(i_{dr}, i_{qr}, \varphi_{dr}, \varphi_{qr}, \omega\right) = (x_1, x_2, x_3, x_4, x_5)$

The system (6) is then written in the form:

$$\dot{x} = f(x) + g(x)u \quad (7)$$

Where

$$f(x) = \begin{cases} \frac{dx_1}{dt} = f_1(x) + a_3 v_{dr} \\ \frac{dx_2}{dt} = f_2(x) + a_3 v_{qr} \\ \frac{dx_3}{dt} = f_3(x) + v_{dr} \\ \frac{dx_4}{dt} = f_4(x) + v_{qr} \\ \frac{dx_5}{dt} = f_5(x) \end{cases} \quad (8)$$

$$u = \left[v_{qr}\ v_{dr}\right]^T ; g(x) = \begin{bmatrix} a_3 & 0 & 1 & 0 & 0 \\ 0 & a_3 & 0 & 1 & 0 \end{bmatrix}^T \quad (9)$$

And

$f_1(x) = -a_1 x_1 + \omega_s x_2 + a_2 x_3 - a_3 x_5 x_4 - a_4 v_{ds}$
,$f_2(x) = -\omega_s x_1 - a_1 x_2 + a_2 x_4 + a_3 x_5 x_3 - a_4 v_{qs}$
$f_3(x) = -b x_1 + \omega_s x_4 - x_5 x_4$, $f_4(x) = -b x_2 - \omega_s x_3 + x_5 x_3$
$f_5(x) = C_1(x_4 x_1 - x_3 x_2) + C_2(C_G - C_{vis})$

3. FEEDBACK LINEARIZATION CONTROL

To develop nonlinear control of the active and reactive powers of stator, the feedback linearization strategy is proposed. This technique consists to transform nonlinear systems into linear ones, so that linear control techniques can be applied. This technique is possible through change of variables and by choosing a suitable control input [17].According to the model of the DFIG developed above, and recalling that the reference is chosen so that its component (d) coincides with the stator voltage vector, this system has as input variables the voltage applied to the rotor ($v_{dr} v_{qr}$) and as output variables the active and reactive power at the stator (P_s, Q_s) defined by:

$$\begin{cases} P_s = v_{qs} i_{qs} + v_{ds} i_{ds} \\ Q_s = v_{qs} i_{ds} - v_{ds} i_{qs} \end{cases} \quad (10)$$

The stator powers' control law is computed according to the rotor current measurement and estimated rotor flux. The latter comes from the proposed high gain observer. Substituting i_{ds} and i_{qs} in (10) by their counterparts extracted from the two last equations of (4), one has:

$$\begin{cases} P_s = v_{qs}(\frac{\varphi_{qr} - L_r I_{qr}}{M}) + v_{ds}(\frac{\varphi_{dr} - L_r I_{dr}}{M}) \\ Q_s = v_{qs}(\frac{\varphi_{dr} - L_r I_{dr}}{M}) - v_{ds}(\frac{\varphi_{qr} - L_r I_{qr}}{M}) \end{cases} \quad (11)$$

Arranging (11)

$$\begin{cases} P_s = \frac{\varphi_{qr}}{M} v_{qs} - \frac{L_r I_{qr}}{M} v_{qs} + \frac{\varphi_{dr}}{M} v_{ds} - \frac{L_r I_{dr}}{M} v_{ds} \\ Q_s = \frac{\varphi_{dr}}{M} v_{qs} - \frac{L_r I_{dr}}{M} v_{qs} - \frac{\varphi_{qr}}{M} v_{ds} + \frac{L_r I_{qr}}{M} v_{ds} \end{cases} \quad (12)$$

Differentiating (12) until an input appears

$$\begin{cases} \dot{P_s} = \frac{\dot{x_4}}{M} v_{qs} - \frac{L_r \dot{x_2}}{M} v_{qs} + \frac{\dot{x_3}}{M} v_{ds} - \frac{L_r \dot{x_1}}{M} v_{ds} \\ \dot{Q_s} = \frac{\dot{x_3}}{M} v_{qs} - \frac{L_r \dot{x_1}}{M} v_{qs} - \frac{\dot{x_4}}{M} v_{ds} + \frac{L_r \dot{x_2}}{M} v_{ds} \end{cases} \quad (13)$$

Write the last equation as follows

$$\begin{cases} \dot{P_s} = \frac{(f_3 - L_r f_1)}{M} v_{ds} + \frac{(f_4 - L_r f_2)}{M} v_{qs} + \frac{(1 - a_3 L_r)}{M} v_{ds} v_{dr} + \frac{(1 - a_3 L_r)}{M} v_{qs} v_{qr} \\ \dot{Q_s} = \frac{(L_r f_2 - f_4)}{M} v_{ds} + \frac{(f_3 - L_r f_1)}{M} v_{qs} + \frac{(1 - a_3 L_r)}{M} v_{qs} v_{dr} + \frac{(a_3 L_r - 1)}{M} v_{ds} v_{qr} \end{cases} \quad (14)$$

It is desired to regulate the output quantities P_s and Q_s to their respective reference value P_{sref} and Q_{sref}

For this purpose defining the adjustment errors

$$\begin{cases} e_1 = P_{sref} - P_s \\ e_2 = Q_{sref} - Q_s \end{cases} \quad (15)$$

Defining the input of the DFIG system

$$u = [u_1 \; u_2]^T = [v_{qr} \; v_{dr}]^T \quad (16)$$

Rewriting (14) in the matrix form

$$\begin{bmatrix} \dot{P_s} \\ \dot{Q_s} \end{bmatrix} = \begin{bmatrix} \frac{(f_3 - L_r f_1)}{M} v_{ds} + \frac{(f_4 - L_r f_2)}{M} v_{qs} \\ \frac{(L_r f_2 - f_4)}{M} v_{ds} + \frac{(f_3 - L_r f_1)}{M} v_{qs} \end{bmatrix} + \begin{bmatrix} \frac{(1 - a_3 L_r)}{M} v_{qs} & \frac{(1 - a_3 L_r)}{M} v_{ds} \\ \frac{(a_3 L_r - 1)}{M} v_{ds} & \frac{(1 - a_3 L_r)}{M} v_{qs} \end{bmatrix} \begin{bmatrix} u_1 \\ u_2 \end{bmatrix} \quad (17)$$

Rewriting the new inputs V_1 and V_2 in the form (18)

$$\begin{cases} \dot{P_s} = V_1 \\ \dot{Q_s} = V_2 \end{cases} \quad (18)$$

From (19) we can write

$$\begin{bmatrix} P_s \\ Q_s \end{bmatrix} = \begin{bmatrix} \frac{1}{s} & 0 \\ 0 & \frac{1}{s} \end{bmatrix} \begin{bmatrix} V_1 \\ V_2 \end{bmatrix} \quad (19)$$

From (17) and (18) the control law is given as

$$\begin{bmatrix} v_{dr} \\ v_{qr} \end{bmatrix} = E(x)^{-1} \left[-A(x) \quad + \begin{bmatrix} V_1 \\ V_2 \end{bmatrix} \right] \quad (20)$$

where

$$A(x) = \begin{bmatrix} \frac{(f_3 - L_r f_1)}{M} v_{ds} + \frac{(f_4 - L_r f_2)}{M} v_{qs} \\ \frac{(L_r f_2 - f_4)}{M} v_{ds} + \frac{(f_3 - L_r f_1)}{M} v_{qs} \end{bmatrix} \text{ and } E(x) = \begin{bmatrix} \frac{(1 - a_3 L_r)}{M} v_{qs} & \frac{(1 - a_3 L_r)}{M} v_{ds} \\ \frac{(a_3 L_r - 1)}{M} v_{ds} & \frac{(1 - a_3 L_r)}{M} v_{qs} \end{bmatrix}$$

The reference active power Ps is generated by MPPT and the reactive power Qs is defined by the grid to support the network voltage .To follow the trajectory of P^*_{sref} and Q^*_{sref} , we use a PI controller imposed to the linearized system [17]. The new input v is given by

$$\begin{bmatrix} V_1 \\ V_2 \end{bmatrix} = \begin{bmatrix} \dot{P}^*_{sref} - k_{p1}e_1 - k_{i1}\int e_1 dt \\ \dot{Q}^*_{sref} - k_{p2}e_2 - k_{i2}\int e_2 dt \end{bmatrix} \quad (21)$$

4. HIGH GAIN OBSERVER FOR FLUX ESTIMATION

We intend to construct such an observer, based on the measurement of the rotor currents, speed and voltages [15] the principle is shown in Figure 3.

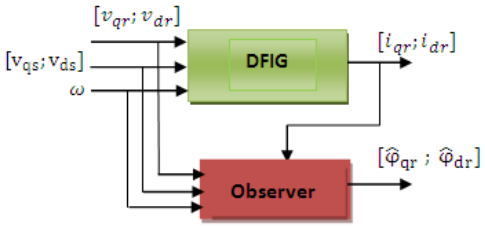

Figure 3. Rotor flux observation strategy.

The estimated flux components $(\hat{\varphi}_{dr}, \hat{\varphi}_{qr})$ are used in the computation of the FBL law.We propose to implement a rotor flux observer in order to study its properties.

From the model (7) and assuming the constant velocity ($\dot{\Omega} = 0$), with $\Omega = \frac{\omega}{p}$ we can write:

$$\dot{X} = A(\Omega)X + Bv \quad (22)$$

where

$$X = \begin{bmatrix} i_{rd}\ i_{rq}\ \varphi_{dr}\ \varphi_{qr} \end{bmatrix} \quad (23)$$

$A(\Omega)$, B and v are given by

$$v = \begin{bmatrix} v_{sd}\ v_{sq}\ v_{rd} v_{rq} \end{bmatrix}^T \quad (24)$$

$$A(\Omega) = \begin{bmatrix} -a_1 & \omega_s & a_2 & -pa_3\Omega \\ \omega_s & -a_1 & pa_3\Omega & a_2 \\ -R_r & 0 & 0 & \omega_s - p\Omega \\ 0 & -R_r & -(\omega_s - p\Omega) & 0 \end{bmatrix}; B = \begin{bmatrix} -a_4 & 0 & a_3 & 0 \\ 0 & -a_4 & 0 & a_3 \\ 0 & 0 & 1 & 0 \\ 0 & 0 & 0 & 1 \end{bmatrix} \quad (25)$$

Thus, at constant Ω, the model is linear, which is a particular case of the form of injection of the output and of the output derivative.

In this part, we are interested in the work presented in [18, 19] which deal with the synthesis of observers with high gain for locally observable systems.

Then it is possible to make out the following change of variables:

$$z = \Phi(x) = \begin{bmatrix} h_1 \\ L_{f+vg}(h_1) \end{bmatrix} \quad (26)$$

$$\begin{cases} z_1 = I \\ z_2 = -(a_1\mathfrak{T} + \omega_s\mathfrak{J})I + +(a_2\mathfrak{T} + a_3 p\Omega\mathfrak{J})\varphi \end{cases} \quad (27)$$

For these changes, model (7) takes the following form:

$$\begin{cases} \dot{z_1} = z_2 - a_4 v_s + a_3 v_r \\ \dot{z_2} = -(a_2\mathfrak{T} - \omega_s\mathfrak{J})(z_2 - a_4 v_s + a_3 v_r) + \\ \quad (a_2\mathfrak{T} + a_3 p\Omega\mathfrak{J})[-R_r z_1 \\ -(\omega_s - p\Omega)\mathfrak{J}(a_2\mathfrak{T} + a_3 p\Omega\mathfrak{J})^{-1}[z_2 - (a_1\mathfrak{T} + \omega_s\mathfrak{J})z_1] + v_r] \end{cases} \quad (28)$$

We put

$$z = \begin{bmatrix} z_1 \\ z_2 \end{bmatrix} \; z_1 = \begin{bmatrix} i_{rd} \\ i_{rq} \end{bmatrix} \; z_2 = \begin{bmatrix} \varphi_{rd} \\ \varphi_{rq} \end{bmatrix} \; \mathcal{A} = \begin{bmatrix} 0 & \mathfrak{T} \\ 0 & 0 \end{bmatrix} \text{ with } = \begin{bmatrix} 1 & 0 \\ 0 & 1 \end{bmatrix}; \mathfrak{J} = \begin{bmatrix} 0 & 1 \\ -1 & 0 \end{bmatrix};$$

$$\psi(v_s, v_r, \Omega, z) = \begin{bmatrix} \psi_i(v_s, v_r, \Omega, z_1) \\ \psi_\varphi(v_s, v_r, \Omega, z_1, z_2) \end{bmatrix} \quad (29)$$

$$\begin{cases} \psi_i(v_s, v_r, \Omega, z_1) = -a_4 v_s + a_3 v_r \\ \psi_\varphi(v_s, v_r, \Omega, z_1, z_2) = \dot{z_2} \end{cases} \quad (30)$$

That transforms the nonlinear system (28) into a local system of pyramidal coordinates

$$\begin{cases} \dot{z} = \mathcal{A}z + \psi(v_s, v_r, z) \\ y = Cz \end{cases} \quad (31)$$

With the output vector $C = [\mathfrak{T}, 0]$
Then the following system

$$\dot{\hat{z}} = \mathcal{A}\hat{z} + \psi(\hat{z}, z) - S_\theta^{-1} C^T (C\hat{z} - y) \quad (32)$$

Is exponential observer of the system with S_θ is the matrix defined by

$$S_\theta = S_\theta^T = \begin{bmatrix} \theta^{-1}\mathfrak{T} & -\theta^{-2}\mathfrak{T} \\ -\theta^{-2}\mathfrak{T} & 2\theta^{-3}\mathfrak{T} \end{bmatrix} \quad (33)$$

With $\theta > 0$ Is the unique solution of the following Lyapunov algebraic equation:

$$\theta S_\theta + \mathcal{A}^T S_\theta + S_\theta \mathcal{A} = C^T C \quad (34)$$

4.1. Theorem

The function ψ is globally Lipchitzian with respect to z uniformly with respect to v_s and v_r

$$\|\psi(\hat{z}, v_s, v_r) - \psi(z, v_s, v_r)\| \leq \mathcal{k}\|\hat{z} - z\| \quad (35)$$

4.2. Proof of stability anaylsis and observer convergence

Consider the error

$$e = \hat{z} - z \quad (36)$$

Its dynamics is given by

$$\dot{e} = (\mathcal{A} - S_\theta^{-1} C^T C)e + \psi(\hat{z}, v_s, v_r) - \psi(z, v_s, v_r) \quad (37)$$

Let's consider the following Lyapunov function candidate

$$V(e) = e^T S_\theta e \quad (38)$$

Its derivative is

$$\begin{aligned} \dot{V(e)} &= \dot{e^T} S_\theta e + e^T S_\theta \dot{e} \\ &= \left[e^T(\mathcal{A} - S_\theta^{-1} C^T C)^T + \left(\psi(\hat{z}, v_s, v_r) - \psi(z, v_s, v_r)\right)^T\right] S_\theta e + \\ &\quad e^T S_\theta[(\mathcal{A} - S_\theta^{-1} C^T C)e + \psi(\hat{z}, v_s, v_r) - \psi(z, v_s, v_r)] \end{aligned} \quad (39)$$

$$= e^T[\mathcal{A}^T S_\theta - 2C^T C + S_\theta \mathcal{A}] + 2e^T S_\theta[\psi(\hat{z}, v_s, v_r) - \psi(z, v_s, v_r)]$$

$$\dot{V(e)} = -e^T(\theta S_\theta + C^T C)e + 2e^T S_\theta[\psi(\hat{z}, v_s, v_r) - \psi(z, v_s, v_r)] \quad (40)$$

Using inequality $C^T C > 0$ and theorem (1) we can increase $\dot{V(e)}$ as following:

$$\dot{V(e)} \leq -e^T \theta S_\theta e + 2\hbar e^T S_\theta e$$
$$\leq -(\theta - 2\hbar)V(e) \quad (41)$$

This guarantees the exponential stability of the observer for $\theta > 2\hbar$ this concludes the proof.

4.3. Observer in the initial coordinates

The observation $\hat{x}$ of the state x for the model (7) is obtained by:

$$\hat{x} = \Phi^{-1}(z) \quad (42)$$

That $z = \Phi(x)$ imply $\frac{\partial z}{\partial t} = \frac{\partial \Phi(x)}{\partial x}\frac{\partial x}{\partial t}$

Is a method of synthesizing the observer expressed in x

$$\dot{\hat{x}} = f(x) + g(x, v) - \left(\frac{\partial \Phi(x)}{\partial x}\right)^{-1} S(\theta)^{-1} C^T(C\hat{x} - y) \quad (43)$$

Or in the panoramic form:

$$\begin{bmatrix} \dot{\hat{i}}_{dr} \\ \dot{\hat{i}}_{qr} \\ \dot{\hat{\varphi}}_{dr} \\ \dot{\hat{\varphi}}_{qr} \end{bmatrix} = \begin{bmatrix} -a_1 \hat{i}_{dr} + \omega_s \hat{i}_{qr} + a_2 \hat{\varphi}_{dr} - a_3 p\Omega \hat{\varphi}_{qr} \\ -\omega_s \hat{i}_{dr} - a_1 \hat{i}_{qr} + a_3 p\Omega \hat{\varphi}_{dr} + a_2 \hat{\varphi}_{qr} \\ -R_r \hat{i}_{dr} - (\omega_s + p\Omega)\hat{\varphi}_{qr} \\ -R_r \hat{i}_{qr} + (-\omega_s + p\Omega)\hat{\varphi}_{dr} \end{bmatrix} + \begin{bmatrix} -a_4 & 0 & a_3 & 0 \\ 0 & -a_4 & 0 & a_3 \\ 0 & 0 & 1 & 0 \\ 0 & 0 & 0 & 1 \end{bmatrix} \begin{bmatrix} v_{ds} \\ v_{qs} \\ v_{dr} \\ v_{qr} \end{bmatrix} -$$
$$\begin{bmatrix} 1 & 0 & 0 & 0 \\ 0 & 1 & 0 & 0 \\ -a_1 & \omega_s & a_2 & -a_3 p\Omega \\ -\omega_s & -a_1 & -a_3 p\Omega & a_2 \end{bmatrix}^{-1} \begin{bmatrix} 2\theta & 0 \\ 0 & 2\theta \\ \theta^2 & 0 \\ 0 & \theta^2 \end{bmatrix} \begin{bmatrix} \hat{i}_{dr} - i_{dr} \\ \hat{i}_{qr} - i_{qr} \end{bmatrix} \quad (44)$$

The DFIG control scheme using conventional feedback linearization (CFBL) associated with HGO is shown in Figure4.

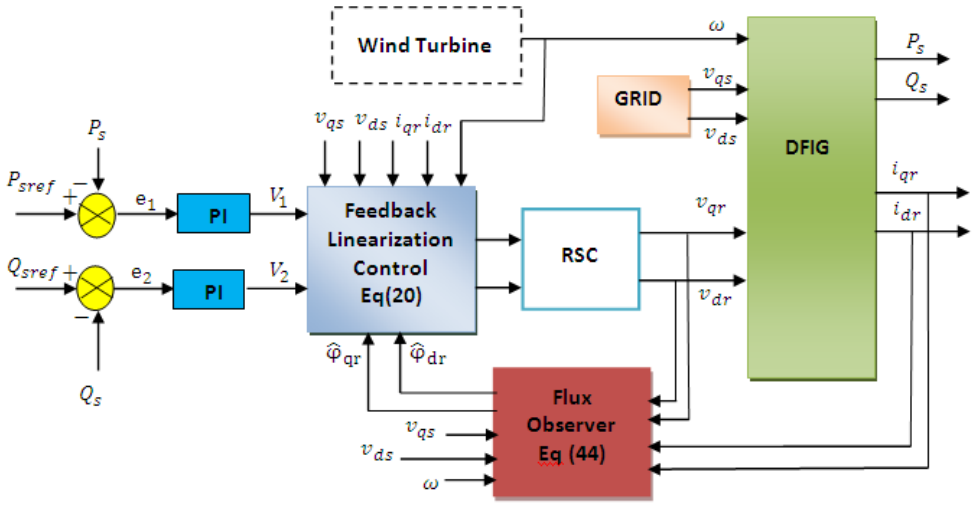

Figure.4.DFIG control scheme using conventional feedback linearization control (CFBL)

5. FUZZY-FEEDBACK LINEARIZATION CONTROL

Fuzzy logic control has been widely used in recent years due to its simplicity of implementation and its ability to control nonlinear systems, which gives better performance under parameter variations and voltage disturbances [20].

Based on the study of fuzzy logic control described in [21], [6] we will proceed to its application to DFIG based on the equation (19) or we consider our system as a simple integrator which facilitates the synthesis of this control where we will have two regulators on each of the loops, that of the active power and that of the reactive power. Figure 5 shows the principle of the proposed method.

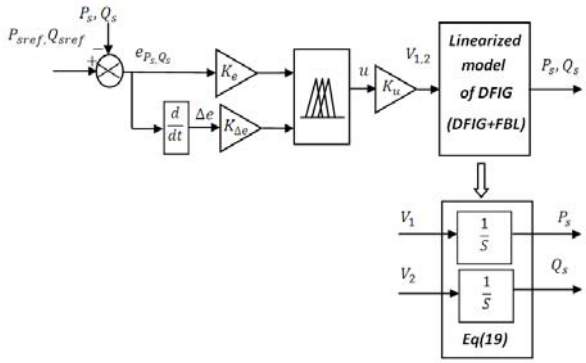

Figure 5. DFIG control scheme using proposed fuzzy-feedback linearization control (PFBL)

The two most significant quantities to analyze the behavior of the system namely the power error e_{P_s,Q_s} and its variation de_{P_s,Q_s} are chosen as two inputs of the regulator by Fuzzy logic controller FLC.

$$\begin{cases} e_{P_s} = P_{sref} - P_s \\ e_{Q_s} = Q_{sref} - Q_s \end{cases} \quad (45)$$

Consider for each variable of measurement (the error and the variation of the error) 3 membership functions noted {N, EZ, P} with: Negative, About Zero, Positive presented in Figure 6.

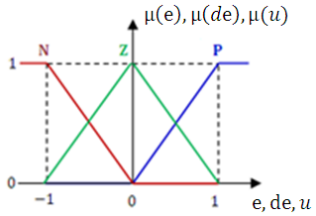

Figure 6. Membership functions

The rule bases of power controller's are illustrated by the following Table 1:

Table 1. Basis of fuzzy control rules

	U	e N	e EZ	e P
de	N	N	N	EZ
	EZ	N	EZ	P
	P	EZ	P	P

For the defuzzification of the output variables of the system, we use the method of the center of gravity (COG) [22].

$$u = \frac{\sum_1^m \mu(x_i).x_i}{\sum_1^m \mu(x_i)} \quad (46)$$

The proposed control is represented in Figure 7.

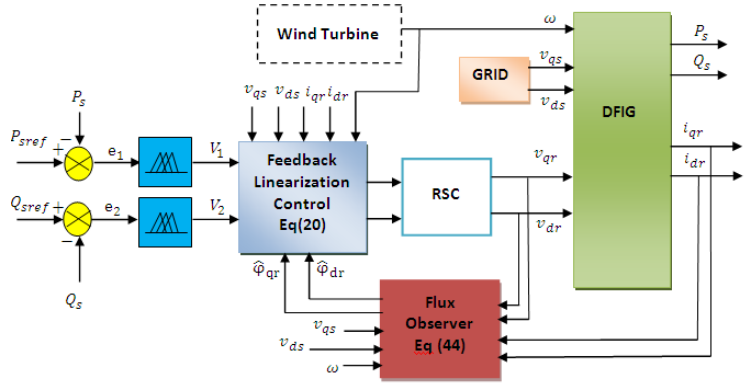

Figure 7. Fuzzy-feedback linearization control combined with high gain observer

6. SIMULATIONS AND RESULTS

In what follows we will study the performances (Reference tracking, disturbance sensitivity and robustness) for different controllers mentioned above conventional feedback linearization control (CFBL) and proposed Fuzzy-Feedback Linearization control (PFBL) using the rotor flux observer.

6.1. Reference tracking

This test consists in making a change in the active and reactive power setp values while maintaining the drive speed of the generator constant. Figure 8 illustrates the behavior of active and reactive powers stator. By examining this figure, it can be seen a good reference tracking with a less ripples for the proposed method compared with the conventional method. The decoupling between the two powers is ideally noted for the proposed method contrary to the conventional method we notice the appearance of a static error at times of step change (see Figure 9). In Figure 10, the observer's performance is illustrated when the estimated rotor fluxes and real fluxes are substantially identical for the dq axis.

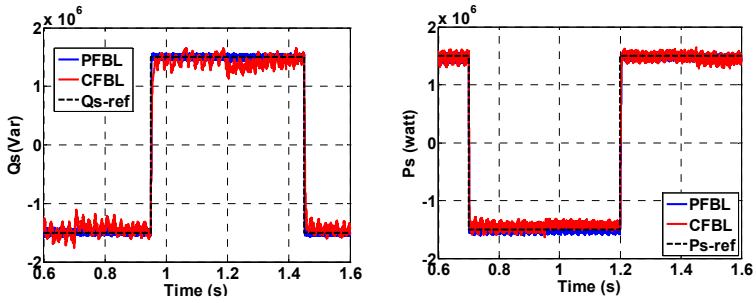

Figure 8. Responses of active and reactive powers

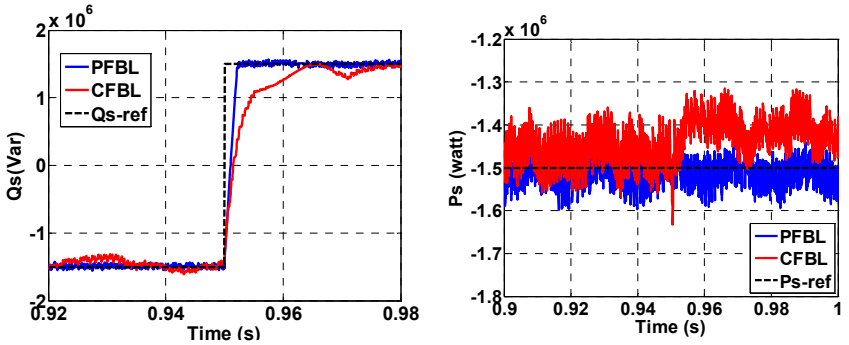

Figure 9. Zoom responses of active and reactive powers

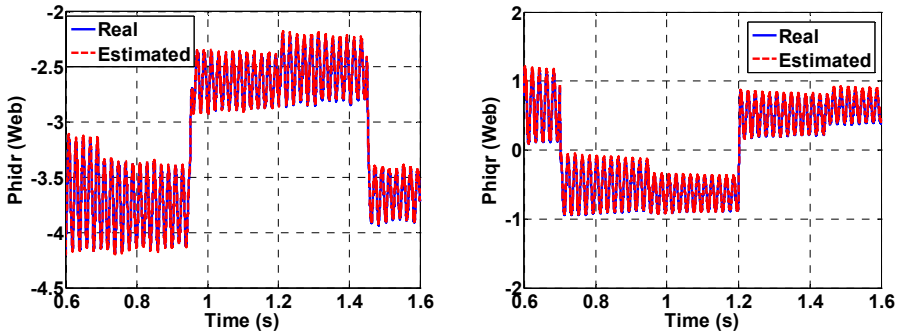

Figure 10. Direct and quadrature flux

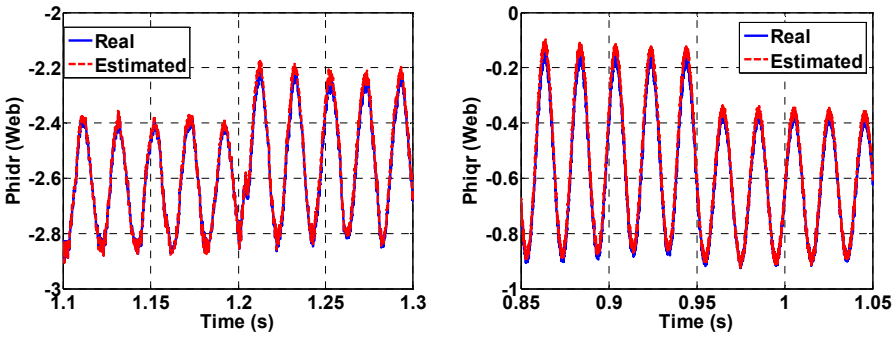

Figure 11. Zoom direct and quadrature flux.

6.2. Disturbance sensitivity

This test use to verify to what extent the measured powers stay at their reference when the grid voltage drops by 20% between 0.8s and 1.3s. The effect of this fault on the active and reactive powers of the machine is illustrated in Figure 12.

The power references are correctly tracked, except for the presence of oscillations which are greatly increased during the fault, the power measurements show a significant deviation from the value of the reference and a reset time greater than 400 ms in the case of a conventional controller compared with the proposed controller which more effectively rejects the voltage drop effects (see Figure 13). The performances of the observer are verified by the simulation results presented in Figure 14. It can be clearly seen that this

voltage drop does not affect the observer because the estimated flux converge to their real values during the fault before stabilizing at steady state (see Figure 15).

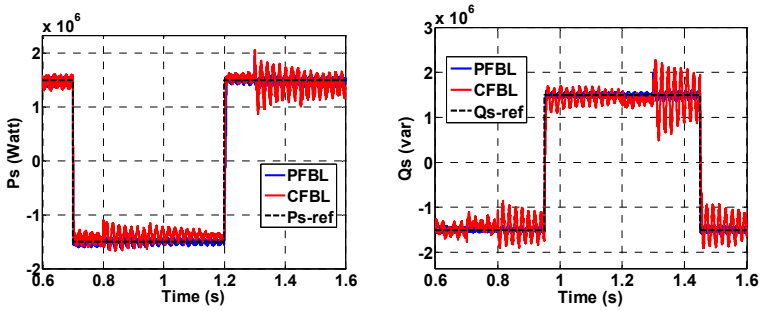

Figure 12. Responses of active and reactive powers during stator voltage drop.

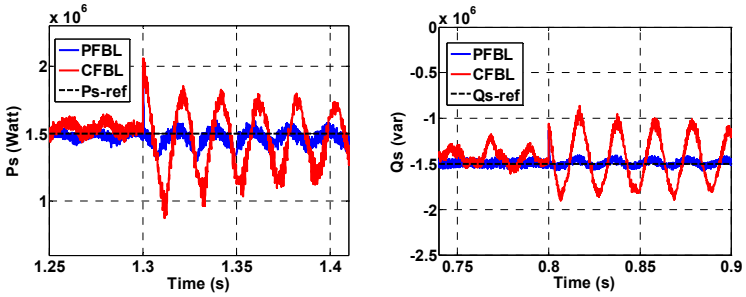

Figure 13. Zoom responses of active and reactive powers during stator voltage

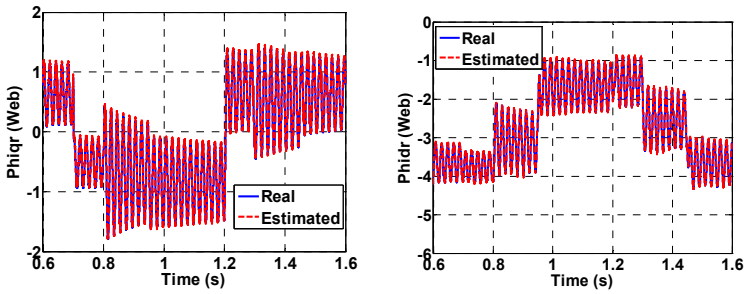

Figure 14. Direct and quadrature flux during stator voltage drop

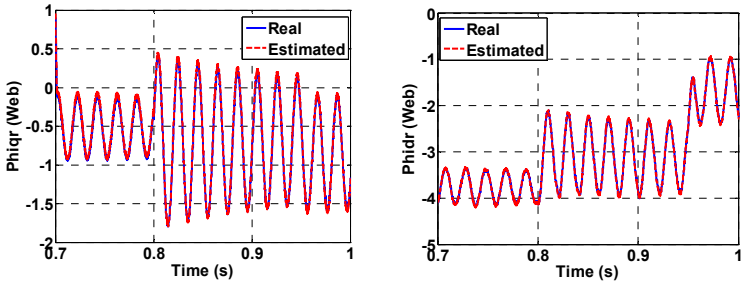

Figure 15. Zoom direct and quadrature flux during stator voltage drop

6.3. Robustness test

Figure 16 shows the evolution of the active and reactive powers during a parametric variation of the generator when the resistance values are increased by 200% and the inductance values decreased by 60%. These results show that the excessive parametric variation caused a clearly degradation of the active and reactive powers curves with the appearance of a static error in the case of the conventional controller. The response of the system with the proposed controller remains insensitive to these variations.

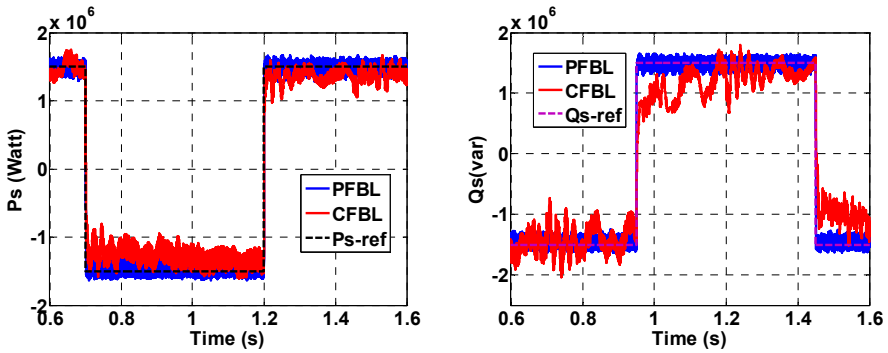

Figure 16. Dynamic responses of active and reactive power under parametric variation of DFIG.

7. CONCLUSION

This work presents a feedback linearization control improvement for a DFIG-based wind system. In this context, we applied the fuzzy logic controller to the feedback linearization strategy. This is intended to improve the performance of the system particularly against parametric uncertainties and disturbance sensitivity that have an effect on conventional feedback linearization control used PI. From the comparative results between the two approaches presented, it can be concluded that intelligent controller have significant improvements to dynamic performances over conventional controllers. In addition, a part was reserved for the synthesis of a high-gain observer to reconstruct non-measurable rotor flux components for technical and economic constraints. This observer is tested by numerical simulation in combination with the adopted control that meets the assigned objectives.

APPENDIX

Table.2 Wind Turbine System Parameters

Parameters	value	unit
Nominal Power	1.5	MW
Turbine radius	35.25	m
Gearbox gain	90	
Stator Voltage	398/690	V
Stator frequency	50	Hz
Number of pairs poles	2	
Nominal speed	150	Rad/sec
Stator resistance	0.012	Ω
Rotor resistance	0.021	Ω
Stator inductance	0.0137	H
Rotor inductance	0.0136	H
Mutual inductance	0.0135	H
Inertia	1000	Kg.m2

REFERENCES

[1] M. A. Abdullah et al., "Particle swarm optimization-based maximum power point tracking algorithm for wind energy conversion system," *IEEE International Conference on Power and Energy (PECon)*, pp. 65-70, 2012.
[2] C. Huang, et al. "Maximum power point tracking strategy for large-scale wind generation systems considering wind turbine dynamics," *IEEE Transactions on Industrial Electronics,* vol. 62, no.4, pp. 2530-2539. 2015.
[3] F. Poitiers, "Etude et commande de génératrices asynchrones pour l'utilisation de l'énergie éolienne-machine asynchrone a cage autonome-machine asynchrone a double alimentation reliée au réseau," Thèse de doctorat, Université de Nantes, 2003.

[4] M .El Achkar et al., "Power operating domain of a cascaded doubly fed induction machine," *Mathematics and Computers in Simulation*, vol.130, pp.142-154, 2016.
[5] E. G .Shehata, "Sliding mode direct power control of RSC for DFIGs driven by variable speed wind turbines," *Alexandria Engineering Journal*, vol.54, no. 4, pp.1067-1075, 2015.
[6] A. Dida, & D. B .Attous, "Doubly-fed induction generator drive based WECS using fuzzy logic controller," *Frontiers in Energy*, vol.9, no.3, pp.272-281.2015.
[7] Y. Ihedrane, C. El Bekkali, B. Bossoufi, "Improved Performance of DFIG-generators for Wind Turbines Variable speed", *International Journal of Power Electronics and Drive Systems (IJPEDS)*, Vol. 9, No. 4, pp. 1875-1890, December 2018
[8] A. F. Zohra et al. "Artificial intelligence control applied in wind energy conversion system," *International Journal of Power Electronics and Drive Systems (IJPEDS)*, Vol. 9, No. 2, pp. 571-578 ,June 2018.
[9] Y.Soufi, S. Kahla, & M. Bechouat, "Feedback linearization control based particle swarm optimization for maximum power point tracking of wind turbine equipped by PMSG connected to the grid ," *International journal of hydrogen energy*, vol.41, no.45, pp. 20950-20955.2016.
[10] P. Li, et al. "Nonlinear controller based on state feedback linearization for series-compensated DFIG-based wind power plants to mitigate sub-synchronous control interaction ," *International Transactions on Electrical Energy Systems*, vol.29, no. 1, p. e.2682.2019.
[11] P. Li, et al. "Sliding mode controller based on feedback linearization for damping of sub-synchronous control interaction in DFIG-based wind power plants ," *International Journal of Electrical Power & Energy Systems*, vol.107, no. 1, p.239-250.2019.
[12] L. Djilali, E. N. Sanchez, & M. Belkheiri, "Neural Input Output Feedback Linearization Control of a DFIG based Wind Turbine ," *IFAC-Papers on Line*, vol.50, no.1, pp.11082-11087.2017.
[13] K. Liao et al. "An input–output linearization algorithm-based inter-area damping control strategy for DFIG ," *IEEJ Transactions on Electrical and Electronic Engineering*, vol.13, no.1, pp. 32-37, 2018.
[14] T. L.Van, H. Nguyen, & M. T.Tran, "Feedback-Linearization-Based Direct Power Control of DFIG Wind Turbine Systems under Unbalanced Grid Voltage ," *International Conference on Advanced Engineering Theory and Applications*. Springer, Cham, pp. 830-839.2017
[15] A .Djoudi, et al. "Robust stator currents sensorless control of stator powers for wind generator based on DFIG and matrix converter ," *Electrical Engineering*, vol.99, no.3, pp. 1043-1051.2017.
[16] S. Mensou et al "Performance of a vector control for DFIG driven by wind turbine: real time simulation using DS1104 controller board" *International Journal of Power Electronics and Drive Systems (IJPEDS)*, Vol. 10, no. 2, pp. 1003-1013, June 2019.
[17] G. Chen et al. "Nonlinear control of the doubly fed induction generator by input-output linearizing strategy ," *Electronics and Signal Processing*. Springer, Berlin, Heidelberg. 601-608. 2011.
[18] J.P .Caron, and J.P .Hautier. "Modélisation et commande de la machine asynchrone ," Vol. 10. Paris: Technip, 1995.
[19] A. Chouya et al. "Etude et mise en œuvre d'un observateur à grand gain de la machine asynchrone ," 18-19. 2006.
[20] M. Veerachary, T. Senjyu, & K. Uezato, "Neural-network-based maximum-power-point tracking of coupled-inductor interleaved-boost-converter-supplied PV system using fuzzy controller ," *IEEE Transactions on Industrial Electronics*, vol. 50, no.4, pp.749-758, 2003.
[21] A. S.Samosir, H. Gusmedi, , S. Purwiyanti, & E. Komalasari, "Modeling and Simulation of Fuzzy Logic based Maximum Power Point Tracking (MPPT) for PV Application ," *International Journal of Power Electronics and Drive Systems (IJPEDS)*, vol.8, no.3, pp.2088-8708, June 2018.
[22] A.Cheriet, A. Bekri, A. Hazzab, H. Gouabi ,"Expert System Based on Fuzzy Logic: Application on Faults Detection and Diagnosis of DFIG," *International Journal of Power Electronics and Drive Systems (IJPEDS)*, vol.9, no. 3, pp. 1081-1089, September 2018.